THE ASTROPHYSICAL JOURNAL, 552:57–71, 2001 May 1

A POSSIBLE CEPHEID-LIKE LUMINOSITY ESTIMATOR FOR THE LONG GAMMA-RAY BURSTS

DANIEL E. REICHART,[1,2,3] DONALD Q. LAMB,[1] EDWARD E. FENIMORE,[4] ENRICO RAMIREZ-RUIZ,[5]
THOMAS L. CLINE,[6] AND KEVIN HURLEY[7]

Received 2000 April 24; accepted 2001 January 1

ABSTRACT

We present a possible Cepheid-like luminosity estimator for the long gamma-ray bursts based on the variability of their light curves. To construct the luminosity estimator, we use *CGRO*/BATSE data for 13 bursts, *Wind*/Konus data for five bursts, *Ulysses*/GRB data for one burst, and *NEAR*/XGRS data for one burst. Spectroscopic redshifts, peak fluxes, and high-resolution light curves are available for 11 of these bursts; partial information is available for the remaining nine bursts. We find that the isotropic equivalent peak luminosities L of these bursts positively correlate with a rigorously constructed measure V of the variability of their light curves. We fit to these data a model that accommodates both intrinsic scatter (statistical variance) and extrinsic scatter (sample variance). We find that $L \sim V^{3.3^{+1.1}_{-0.9}}$. If one excludes GRB 980425 from the fit, on the grounds that its association with SN 1998bw at a redshift of $z = 0.0085$ is not secure, the luminosity estimator spans ≈ 2.5 orders of magnitude in L, and the slope of the correlation between L and V is positive with a probability of $1 - (1.4 \times 10^{-4})$ ($3.8\ \sigma$). Although GRB 980425 is excluded from this fit, its L and V values are consistent with the fitted model, which suggests that GRB 980425 may well be associated with SN 1998bw and that GRB 980425 and the cosmological bursts may share a common physical origin. If one includes GRB 980425 in the fit, the luminosity estimator spans ≈ 6.3 orders of magnitude in L, and the slope of the correlation is positive with a probability of $1 - (9.3 \times 10^{-7})$ ($4.9\ \sigma$). In either case, the luminosity estimator yields best-estimate luminosities that are accurate to a factor of ≈ 4, or best-estimate luminosity distances that are accurate to a factor of ≈ 2. Regardless of whether GRB 980425 should be included in the fit, its light curve is unique in that it is much less variable than the other ≈ 17 light curves of bursts in our sample for which the signal-to-noise ratio is reasonably good.

Subject heading: gamma rays: bursts

1. INTRODUCTION

Since gamma-ray bursts (GRBs) were first discovered (Klebesadel, Strong, & Olson 1973), thousands of bursts have been detected by a wide variety of instruments, most notably the Burst and Transient Source Experiment (BATSE) on the *Compton Gamma-Ray Observatory* (*CGRO*), which will have detected about 2700 bursts by the end of *CGRO*'s more than nine-year mission in 2000 June (see, e.g., Paciesas et al. 1999). However, the distance scale of the bursts remained uncertain until 1997, when *BeppoSAX* began localizing long bursts to a few arcminutes on the sky and distributing the locations to observers within hours of the bursts. This led to the discovery of X-ray (Costa et al. 1997), optical (van Paradijs et al. 1997), and radio (Frail et al. 1997) afterglows, as well as host galaxies (Sahu et al. 1997). Subsequent observations led to the spectroscopic determination of burst redshifts, using absorption lines in the spectra of the afterglows (see, e.g., Metzger et al. 1997) and emission lines in the spectra of the host galaxies (see, e.g., Kulkarni et al. 1998a). To date, redshifts have been measured for 13 bursts.

Recently, Stern, Poutanen, & Svensson (1999; see also Stern, Svensson, & Poutanen 1997), Norris, Marani, & Bonnell (2000b; see also Norris, Marani, & Bonnell 2000a), and Fenimore & Ramirez-Ruiz (2000; see also Ramirez-Ruiz & Fenimore 1999) have proposed trends for the long bursts between burst luminosity and quantities that can be measured directly from burst light curves. Using 1310 BATSE bursts for which peak fluxes and high-resolution light curves were available, Stern et al. (1999) have suggested that simple bursts (those dominated by a single, smooth pulse) are less luminous than complex bursts (those consisting of overlapping pulses); however, see § 5. Using a sample of seven BATSE bursts for which spectroscopic redshifts, peak fluxes, and high-resolution light curves were available, Norris et al. (2000b) have suggested that more luminous bursts have shorter spectral lags (the interval of time between the peak of the light curve in different energy bands). Using the same seven bursts, Fenimore & Ramirez-Ruiz (2000) have suggested that more luminous bursts have more variable light curves. These trends between luminosity and quantities that can be measured directly from light curves raise the exciting possibility that luminosities, and hence luminosity distances, might be inferred for the long bursts from their light curves alone.

In this paper, we present a possible luminosity estimator for the long bursts, the construction of which was motivated by the work of Ramirez-Ruiz & Fenimore (1999) and Fenimore & Ramirez-Ruiz (2000). We term the luminosity estimator

[1] Department of Astronomy and Astrophysics, University of Chicago, 5640 South Ellis Avenue, Chicago, IL 60637.
[2] Department of Astronomy, California Institute of Technology, Mail Stop 105-24, 1201 East California Boulevard, Pasadena, CA 91125.
[3] Hubble Fellow.
[4] MS D436, Los Alamos National Laboratory, Los Alamos, NM 87545.
[5] Institute of Astronomy, Madingley Road, Cambridge CB3 0HA, England, UK.
[6] NASA Goddard Space Flight Center, Code 661, Greenbelt, MD 20771.
[7] Space Sciences Laboratory, University of California, Berkeley, Berkeley, CA 94720.

"Cepheid-like" in that it can be used to infer luminosities and luminosity distances for the long bursts from the variabilities of their light curves alone. We apply this luminosity estimator to every long burst in the current BATSE catalog in an upcoming paper (Reichart et al. 2001).

We rigorously construct our measure V of the variability of a burst light curve in § 2. Qualitatively, V is computed by taking the difference between the light curve and a smoothed version of the light curve, squaring this difference, summing the squared difference over time intervals, and appropriately normalizing the result. Our variability measure differs from that of Fenimore & Ramirez-Ruiz (2000) in three important ways: (1) we define the timescale over which the light curve is smoothed differently; (2) we subtract out the contribution to the variability due to Poisson noise differently; and (3) we combine variability measurements of light curves acquired in different energy bands into a single measurement differently.

We find that only smoothing timescales that are proportional to burst duration appear to lead to significant correlations between the isotropic equivalent peak photon luminosity L of a burst and V; in particular, smoothing timescales of a fixed duration in the source frame do not. We take the smoothing timescale of a burst light curve, acquired in observer-frame energy band E, to be the time spanned by the brightest $100f$% of the total counts above background, where f is a number between 0 and 1 that we fix using the data in § 4. We schematically illustrate this measure of duration in Figures 1 and 2. In Figure 1, the 50% smoothing timescale of the light curve is given by $T^E_{f=0.5} = T_1 + T_2$, and the 90% smoothing timescale of the light curve is given by $T^E_{f=0.9} = T_3$; in Figure 2, the 50% smoothing timescale of the light curve is given by $T^E_{f=0.5} = T_4$, and the 90% smoothing timescale of the light curve is given by $T^E_{f=0.9} = T_5 + T_6$. We have chosen this measure of the smoothing timescale over others because it is robust: small variations in either the light curve or the value of f result in only small variations in the value of the smoothing timescale. This is not the case with measures like T_{50} and T_{90} (see, e.g., Paciesas et al. 1999).

For example, consider the case of a burst with a precursor. The value of T_{90}, for example, can differ considerably depending on whether the precursor accounts for more than 5% of the total counts above background or less. Likewise, if the precursor's counts above background is, e.g., 5% of the total, the duration measured using $T_{<90}$ can differ considerably from that using $T_{>90}$. The effect of using an artificially long (short) smoothing timescale is measuring an artificially high (low) variability. Our measure of the smoothing timescale does not suffer from such robustness problems.

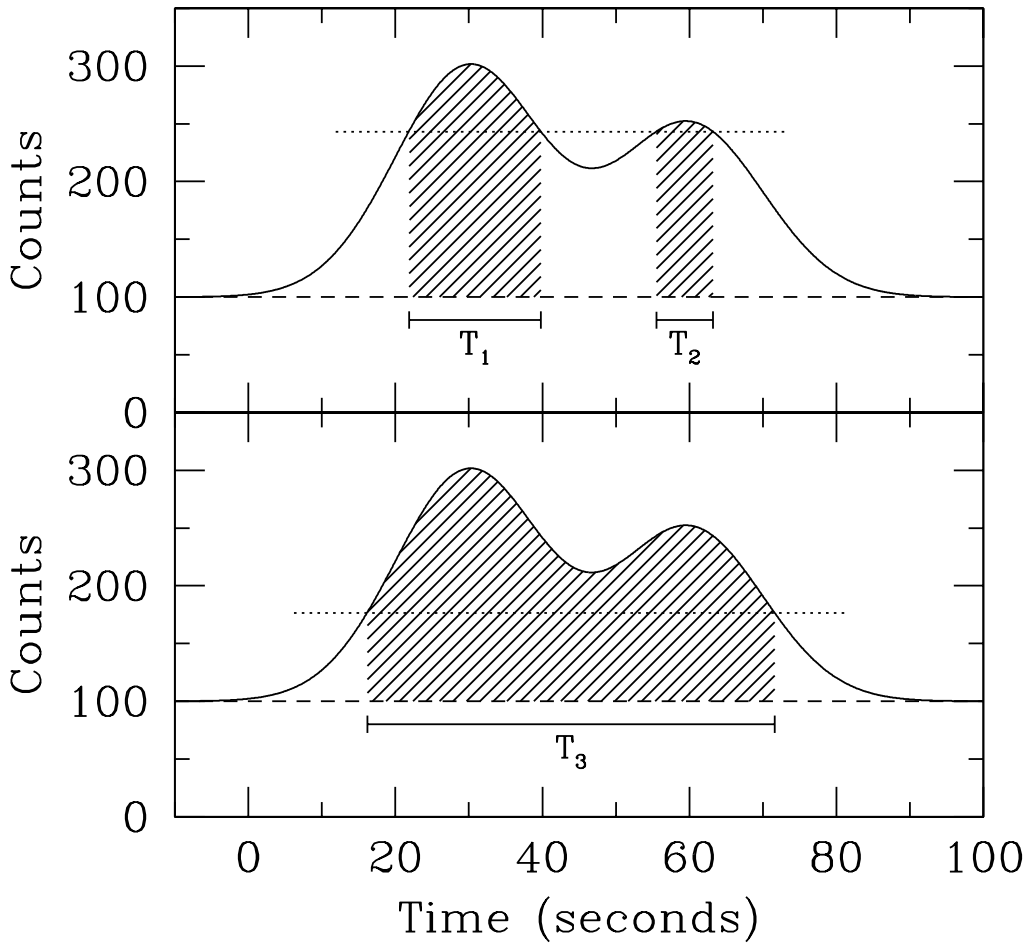

FIG. 1.—Schematic illustration of our measure of burst duration. The solid line represents a burst light curve acquired in observer-frame energy band E, and the dashed line represents the background. *Top*: Hatched area is the brightest 50% of the total counts above background. Hence, the 50% duration, or smoothing timescale, of this light curve is given by $T^E_{f=0.5} = T_1 + T_2$. *Bottom*: Hatched area is the brightest 90% of the total counts above background. Hence, the 90% duration, or smoothing timescale, of this light curve is given by $T^E_{f=0.9} = T_3$.

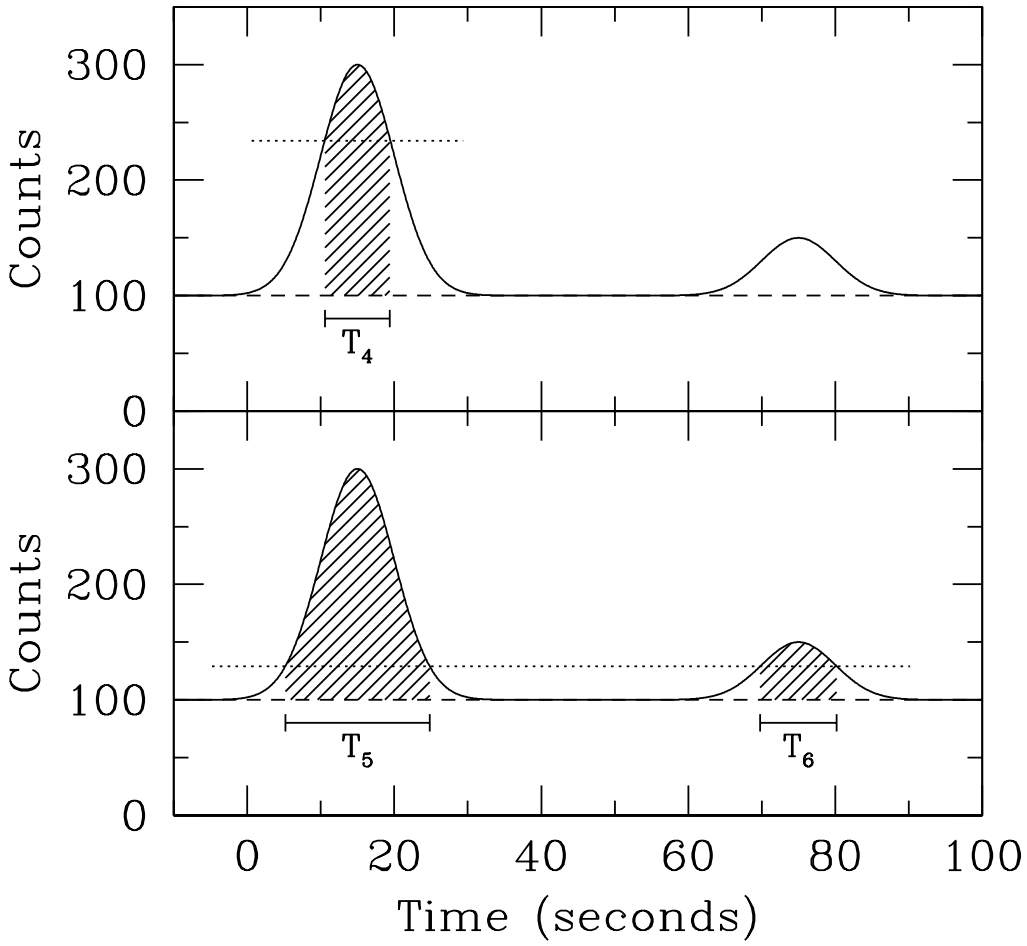

FIG. 2.—Another schematic illustration of our measure of burst duration. The solid line represents a burst light curve acquired in observer-frame energy band E, and the dashed line represents the background. *Top*: Hatched area is the brightest 50% of the total counts above background. Hence, the 50% duration, or smoothing timescale, of this light curve is given by $T^E_{f=0.5} = T_4$. *Bottom*: Hatched area is the brightest 90% of the total counts above background. Hence, the 90% duration, or smoothing timescale, of this light curve is given by $T^E_{f=0.9} = T_5 + T_6$.

We present our measure of the isotropic equivalent peak photon luminosity L of a burst in § 3. In § 4, we expand the original Ramirez-Ruiz & Fenimore (1999) sample of seven bursts to include a total of 20 bursts, including 13 BATSE bursts, five *Wind*/Konus bursts, one *Ulysses*/GRB burst, and one *NEAR*/XGRS burst. Spectroscopic redshifts, peak fluxes, and high-resolution light curves are available for 11 of these bursts; partial information is available for the remaining nine bursts.

Also in § 4, we construct our luminosity estimator, which differs from that of Fenimore & Ramirez-Ruiz (2000) in two important ways: (1) applying the Bayesian inference formalism developed by Reichart (2001), we fit a model to the data that accommodates both intrinsic scatter (statistical variance) in two dimensions and extrinsic scatter (sample variance) in two dimensions; (2) again applying this formalism, we determine not only the best estimate for L as a function of V, but also the uncertainty in L as a function of V; in addition, we approximate these functions with analytic expressions. We state our conclusions in § 5.

2. THE VARIABILITY MEASURE

We now rigorously construct a measure of the variability of a burst light curve. We require it to have the following properties: (1) we define it in terms of physical, source-frame quantities, as opposed to measured, observer-frame quantities; (2) when it is converted to observer-frame quantities, all strong dependences on redshift and other difficult or impossible to measure quantities cancel out; (3) it is not biased by instrumental binning of the light curve, despite cosmological time dilation and the narrowing of the light curve's temporal substructure at higher energies (Fenimore et al. 1995); (4) it is not biased by Poisson noise and consequently can be applied to faint bursts; and (5) it is robust, i.e., similar light curves always yield similar variabilities. We also derive an expression for the statistical uncertainty in a light curve's measured variability. Finally, we describe how we combine variability measurements of light curves acquired in different energy bands into a single measurement.

We first define the variability of a burst light curve acquired in observer-frame energy band E in terms of physical, source-frame quantities:

$$V^E_f = \frac{\int_{-\infty}^{\infty} [L^{E_s}(t_s) - (L^{E_s} * S_f)(t_s)]^2 dt_s}{\int_{-\infty}^{\infty} [L^{E_s}(t_s)]^2 dt_s}, \quad (1)$$

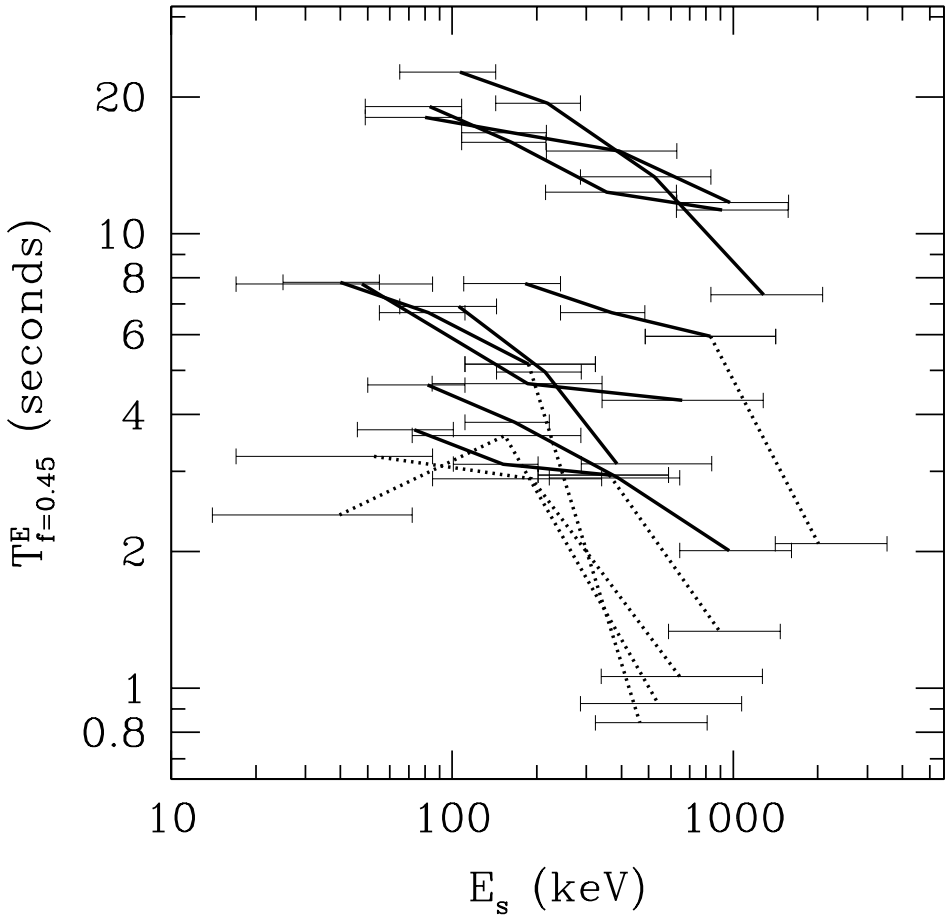

FIG. 3.—Bursts in our sample for which spectroscopic redshifts, peak fluxes, and 64 ms or better resolution light curves are available. For each of these bursts, light curves were acquired in, typically, three or four independent energy bands E. For each burst, we compute the durations, or smoothing timescales, $T^E_{f=0.45}$, of its three or four independent light curves, and plot $T^E_{f=0.45}$ as a function of source-frame energy band $E_s = E(1+z)$. The horizontal bars mark the source-frame energy bands. We plot solid lines if the light curve has more than 3000 total counts above background, and dotted lines if the light curve has fewer than 3000 total counts above background. The dotted portions of these curves suffer from low signal-to-noise ratio; very little variability information can be gleaned from these light curves. However, the trend is clear: the durations, or smoothing timescales, $T^E_{f=0.45}$, of these bursts are shorter at higher energies. From the solid portions of these curves, we find that $T^E_{f=0.45} \sim E^{-0.4}$, in agreement with the principle result of Fenimore et al. (1995). Other values of f yield similar results.

where $L^{E_s}(t_s)$ is the luminosity of the burst in source-frame energy band $E_s = E(1+z)$ as a function of source-frame time t_s and $(L^{E_s} * S_f)(t_s)$ is the convolution of this function with a boxcar smoothing function of area equal to 1 and width equal to the smoothing timescale of $L^{E_s}(t_s)$, i.e., the source-frame smoothing timescale of the light curve. Because our definition of the smoothing timescale is a robust measure of duration (see § 1), equation (1) is a robust measure of variability.

Next, we convert equation (1) to observer-frame quantities:

$$V^E_{f,P} = \frac{\int_{-\infty}^{\infty} \{C^E(t_o) - B^E(t_o) - [(C^E - B^E) * S_f](t_o)\}^2 [\Delta\Omega D^2(z)(1+z)^{\alpha}]^2 (1+z)^{\beta} dt_o}{\int_{-\infty}^{\infty} [C^E(t_o) - B^E(t_o)]^2 [\Delta\Omega D^2(z)(1+z)^{\alpha}]^2 (1+z)^{\beta} dt_o} . \quad (2)$$

Here $C^E(t_o)$ and $B^E(t_o)$ are the total (source plus background) and background photon count rates in observer-frame energy band E as a function of observer-frame time t_o, $[(C^E - B^E) * S_f](t_o)$ is the convolution of $C^E(t_o) - B^E(t_o)$ with a boxcar smoothing function of area equal to 1 and width equal to the smoothing timescale of $C^E(t_o) - B^E(t_o)$, i.e., T^E_f, $\Delta\Omega$ is the effective solid angle of the emitted light, $D(z)$ is the comoving distance to the burst at redshift z, α is either 1 or 2 depending on whether $L^{E_s}(t_s)$ is a photon number or energy luminosity, and $\beta \approx 1 - 0.4 = 0.6$: the factor of $(1+z)^1$ is due to cosmological time dilation, and the factor of $\approx (1+z)^{-0.4}$ is due to the narrowing of the light curve's temporal substructure at higher energies (Fenimore et al. 1995). By construction, the strong dependences on $\Delta\Omega$, z, α, and β and a weak dependence on the cosmological model cancel out. Furthermore, since $B^E(t_o)$ always varies over much longer timescales than T^E_f, equation (2) simplifies to

$$V^E_{f,P} = \frac{\int_{-\infty}^{\infty} [C^E(t_o) - (C^E * S_f)(t_o)]^2 dt_o}{\int_{-\infty}^{\infty} [C^E(t_o) - B^E(t_o)]^2 dt_o} . \quad (3)$$

We distinguish equations (2) and (3) from equation (1) with a subscript P because they differ in one fundamental way: unlike $L^{E_s}(t_s)$ in equation (1), $C^E(t_o)$ suffers from Poisson noise. This additional source of variability biases equations (2) and (3) toward

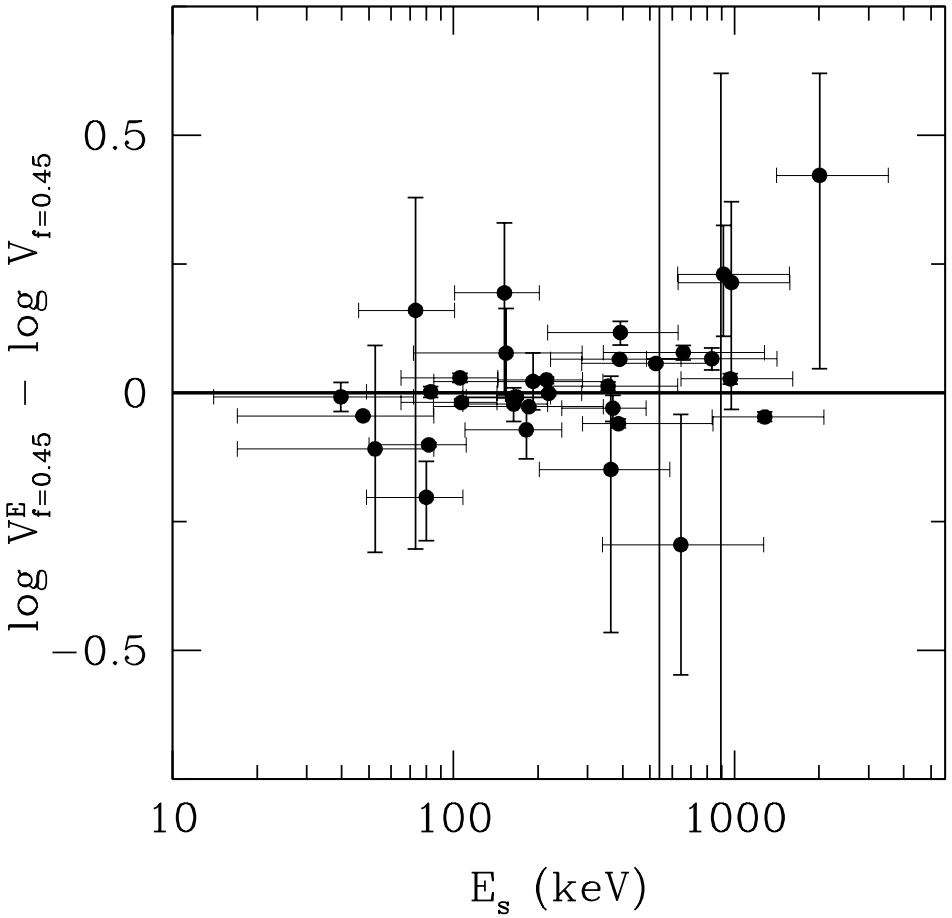

FIG. 4.—Bursts in our sample for which spectroscopic redshifts, peak fluxes, and 64 ms or better resolution light curves are available. For each of these bursts, light curves were acquired in, typically, three or four independent energy bands E. For each burst, we compute the variabilities $V^E_{f=0.45}$ of its three or four independent light curves, and the combined variability $V_{f=0.45}$ of the burst. We plot $\log V^E_{f=0.45} - \log V_{f=0.45}$ vs. source-frame energy band $E_s = E(1+z)$. The horizontal bars mark the source-frame energy bands. Clearly, there is no significant trend with energy. Other values of f yield similar results.

higher values. Although this bias is minor for bursts that are significantly brighter than the background, it cannot be ignored for faint bursts. We determine and subtract out the contribution to the variability due to Poisson noise below.

However, before we can subtract out the contribution to the variability due to Poisson noise, we must first bin the light curve, because observed light curves are typically discrete, not continuous. Consequently, we replace the integrals in equation (3) with sums from $i = 1$ to N, $C^E(t_o)$ with C^E_i, $B^E(t_o)$ with B^E_i, and $(C^E * S_f)(t_o)$ with its discrete equivalent, $S_i(C^E_j, N^E_f)$. Here, C^E_j is the light curve to be smoothed, N^E_f is the smoothing timescale, i.e., T^E_f, but measured in number of bins, and

$$S_i(C^E_j, N_x) = \frac{1}{N_x}\left[\sum_{j=i-n_x}^{i+n_x} C^E_j + \left(\frac{N_x - 1}{2} - n_x\right)(C^E_{i-n_{x-1}} + C^E_{i+n_{x+1}})\right], \tag{4}$$

where n_x is the truncated integer value of $(N_x - 1)/2$. Binning can bias the variability measure, because binning wipes out all variability on timescales shorter than the sampling timescale of the light curve, and the effective sampling timescale of the light curve in the source frame decreases with increasing burst redshift: although the sampling timescale of the light curve is fixed by the instrument in the observer frame, both cosmological time dilation and the narrowing of the light curve's temporal substructure at higher energies (Fenimore et al. 1995) decrease the effective sampling timescale of the light curve in the source frame. We remove this redshift bias by smoothing all light curves on a source-frame timescale of 64 ms (the shortest sampling timescale of BATSE), which corresponds to a timescale of $64(1+z)^\beta$ ms in the observer frame. Consequently, we replace C^E_i with $S_i(C^E_j, N_z)$, where $N_z = 64(1+z)^\beta/\Delta t$, and Δt is the observer-frame sampling timescale of the light curve in milliseconds. Equation (3) becomes

$$V^E_{f,P} = \frac{\sum_{i=1}^{N} [S_i(C^E_j, N_z) - S_i(C^E_j, N^E_f)]^2}{\sum_{i=1}^{N} [S_i(C^E_j, N_z) - B^E_i]^2}, \tag{5}$$

where we take C^E_j and B^E_i to be measured in counts, not counts per unit time. Although the computation of $V^E_{f,P}$ now depends on z and β, these dependences are very weak: wide variations in the values of these parameters do not significantly change the measured variabilities of the bursts in our sample; i.e., burst light curves have very little power on such short timescales. Likewise, wide variations in the value of the effective sampling timescale of the light curve that we impose in the source frame also have little effect on the measured variabilities of these bursts.

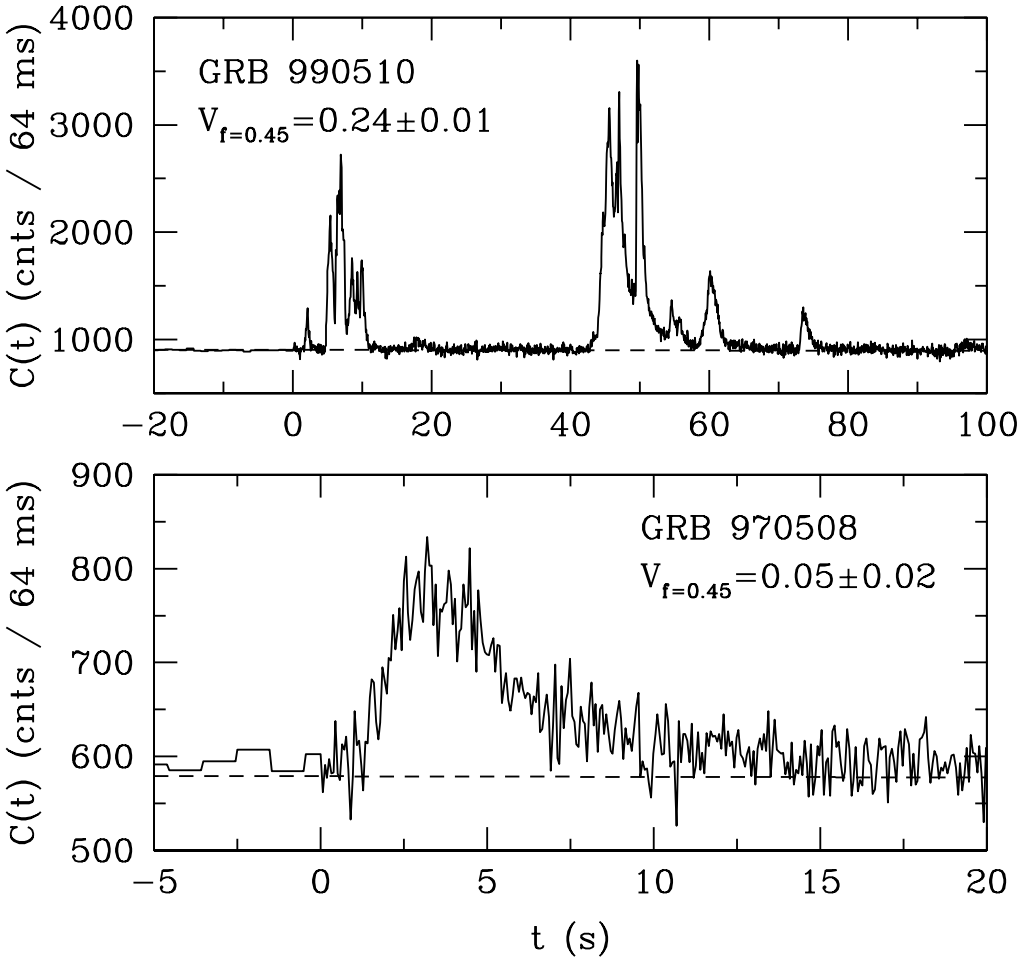

FIG. 5.—The >25 keV light curves of the most (GRB 990510) and least (GRB 970508) variable cosmological BATSE bursts in our sample. In the case of GRB 990510 ($z = 1.619$), we find that $V_{f=0.45} = 0.24 \pm 0.01$. In the case of GRB 970508 ($z = 0.835$), we find that $V_{f=0.45} = 0.05 \pm 0.02$.

Now we determine and subtract out the contribution of Poisson noise to the variability, and we simultaneously derive an expression for the statistical uncertainty in a light curve's measured variability. First, we rewrite the expressions $S_i(C_j^E, N_z) - S_i(C_j^E, N_f^E)$ and $S_i(C_j^E, N_z) - B_i^E$ from equation (5) as weighted sums of the statistically independent measurements C_j:

$$V_{f,P}^E = \frac{\sum_{i=1}^N (\sum_{j=1}^N a_{ij} C_j)^2}{\sum_{i=1}^N (\sum_{j=1}^N b_{ij} C_j - B_i)^2}, \tag{6}$$

where a_{ij} and b_{ij} are weights that differ for each burst but can be computed straightforwardly using equation (4). Since we are in the Gaussian limit, the uncertainty in each C_j is simply $\pm\sqrt{C_j}$. Since each C_j is statistically independent, their weighted uncertainties can be summed in quadrature. Hence, the sums over j in equation (6) and their uncertainties are $\sum_{j=1}^N a_{ij} C_j \pm (\sum_{j=1}^N a_{ij}^2 C_j)^{1/2}$ and $\sum_{j=1}^N b_{ij} C_j - B_i \pm (\sum_{j=1}^N b_{ij}^2 C_j)^{1/2}$.

Next, in accordance with equation (6), we square these expressions, which yields expressions consisting of three terms: the square of the original term, a positive term due to Poisson noise, and an uncertainty term. Subtracting out the contributions to equation (6) due to Poisson noise yields

$$V_f^E = \frac{\sum_{i=1}^N [(\sum_{j=1}^N a_{ij} C_j)^2 - \sum_{j=1}^N a_{ij}^2 C_j]}{\sum_{i=1}^N [(\sum_{j=1}^N b_{ij} C_j - B_i)^2 - \sum_{j=1}^N b_{ij}^2 C_j]}, \tag{7}$$

where the uncertainty in the ith term of the numerator is $\pm 2(\sum_{j=1}^N a_{ij} C_j)(\sum_{j=1}^N a_{ij}^2 C_j)^{1/2}$, and the uncertainty in the ith term of the denominator is $\pm 2(\sum_{j=1}^N b_{ij} C_j - B_i)(\sum_{j=1}^N b_{ij}^2 C_j)^{1/2}$. Recognizing that only $\approx N/N_z$ of the terms in the sums over i are statistically independent, since the sums over j correspond to a convolution of the light curve with a boxcar smoothing function of width equal to N_z bins, the uncertainties in the sums over i are a factor of $\approx \sqrt{N_z}$ larger than what would be derived if all of the terms were statistically independent. Hence, the uncertainty in the numerator is $\approx \pm 2 [N_z \sum_{i=1}^N (\sum_{j=1}^N a_{ij} C_j)^2 \sum_{j=1}^N a_{ij}^2 C_j]^{1/2}$, and the uncertainty in the denominator is $\approx \pm 2 [N_z \sum_{i=1}^N (\sum_{j=1}^N b_{ij} C_j - B_i)^2 \sum_{j=1}^N b_{ij}^2 C_j]^{1/2}$. These uncertainties can be at most only weakly correlated. Taking them to be independent, we find that the statistical uncertainty in a light curve's measured variability is approximately given by

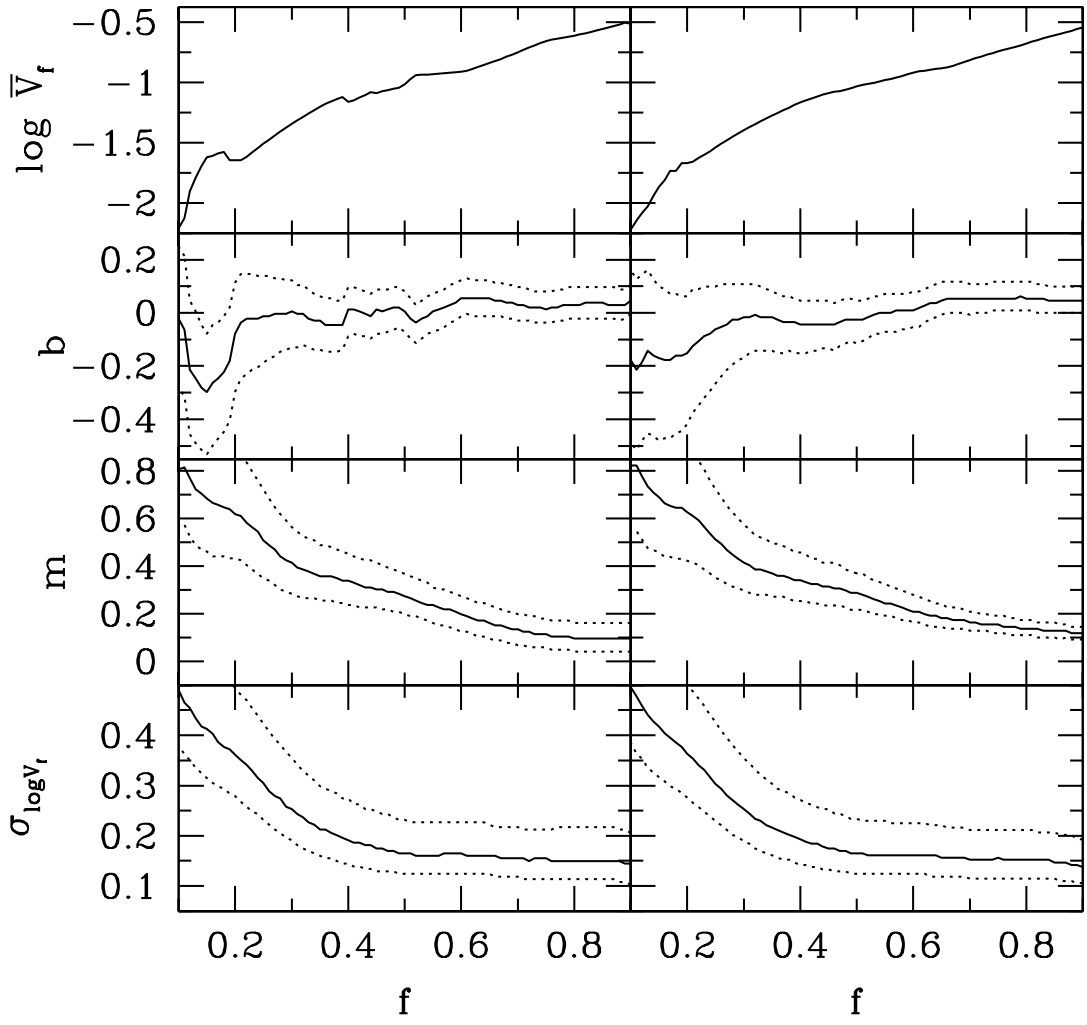

FIG. 6.—Value of $\log \bar{V}_f$ as a function of f and the best-fit values and 1 σ uncertainties in the best-fit values of the model parameters b, m, and $\sigma_{\log V_f}$ as functions of f. In the left panels, we exclude GRB 980425 from the fits; in the right panels we include GRB 980425 in the fits.

$$\sigma_{V_f{}^E} = V_f^E \sqrt{\frac{4N_z \sum_{i=1}^{N} (\sum_{j=1}^{N} a_{ij} C_j)^2 \sum_{j=1}^{N} a_{ij}^2 C_j}{\{\sum_{i=1}^{N} [(\sum_{j=1}^{N} a_{ij} C_j)^2 - \sum_{j=1}^{N} a_{ij}^2 C_j]\}^2} + \frac{4N_z \sum_{i=1}^{N} (\sum_{j=1}^{N} b_{ij} C_j - B_i)^2 \sum_{j=1}^{N} b_{ij}^2 C_j}{\{\sum_{i=1}^{N} [(\sum_{j=1}^{N} b_{ij} C_j - B_i)^2 - \sum_{j=1}^{N} b_{ij}^2 C_j]\}^2}} \,. \tag{8}$$

All that remains is to describe how we combine variability measurements of light curves acquired in different energy bands, V_f^E, into a single measurement of a burst's variability, V_f. For each burst in our sample, light curves were acquired in typically three or four independent energy bands (see Table 2). We find that (1) the smoothing timescales of these light curves decrease with energy as $\approx E^{-0.4}$ (Fig. 3) and (2) the variabilities of these light curves are approximately constant across energy bands (Fig. 4). In hindsight, the former result is not surprising, given our definition of the smoothing timescale and the principle result of Fenimore et al. (1995); however, it does constitute an independent confirmation of their result. Result (2) suggests that we can model a burst's variability as a constant across energy bands. Applying the Bayesian inference formalism developed by Reichart (2001) for fitting models with extrinsic scatter (sample variance) to data with intrinsic scatter (statistical variance, in this case given by eq. [8]), we fit this model to the typically three or four independent measurements of a burst's variability made in independent energy bands, V_f^E, resulting in a single measurement of that burst's variability, V_f, and the uncertainty in V_f. We plot the >25 keV light curves of the most and least variable cosmological BATSE bursts in our sample in Figure 5.

3. THE LUMINOSITY MEASURE

Let P be the peak flux of a burst in photons cm^{-2} s^{-1} between observer-frame energies E_l and E_u. The isotropic equivalent peak photon luminosity of the burst in ergs per second between source-frame energies 100 and 1000 keV is given by

$$L = 4\pi D^2(z) P \frac{\int_{100}^{1000} E\Phi[E/(1+z)]dE}{\int_{E_l}^{E_u} \Phi(E)dE} \,, \tag{9}$$

where $\Phi(E)$ is the observer-frame spectral shape, which we parameterize with the Band function (Band et al. 1993). For each burst in our sample, we compute the value of L for each of the 54 parameterizations of the Band function in Band et al. (1993);

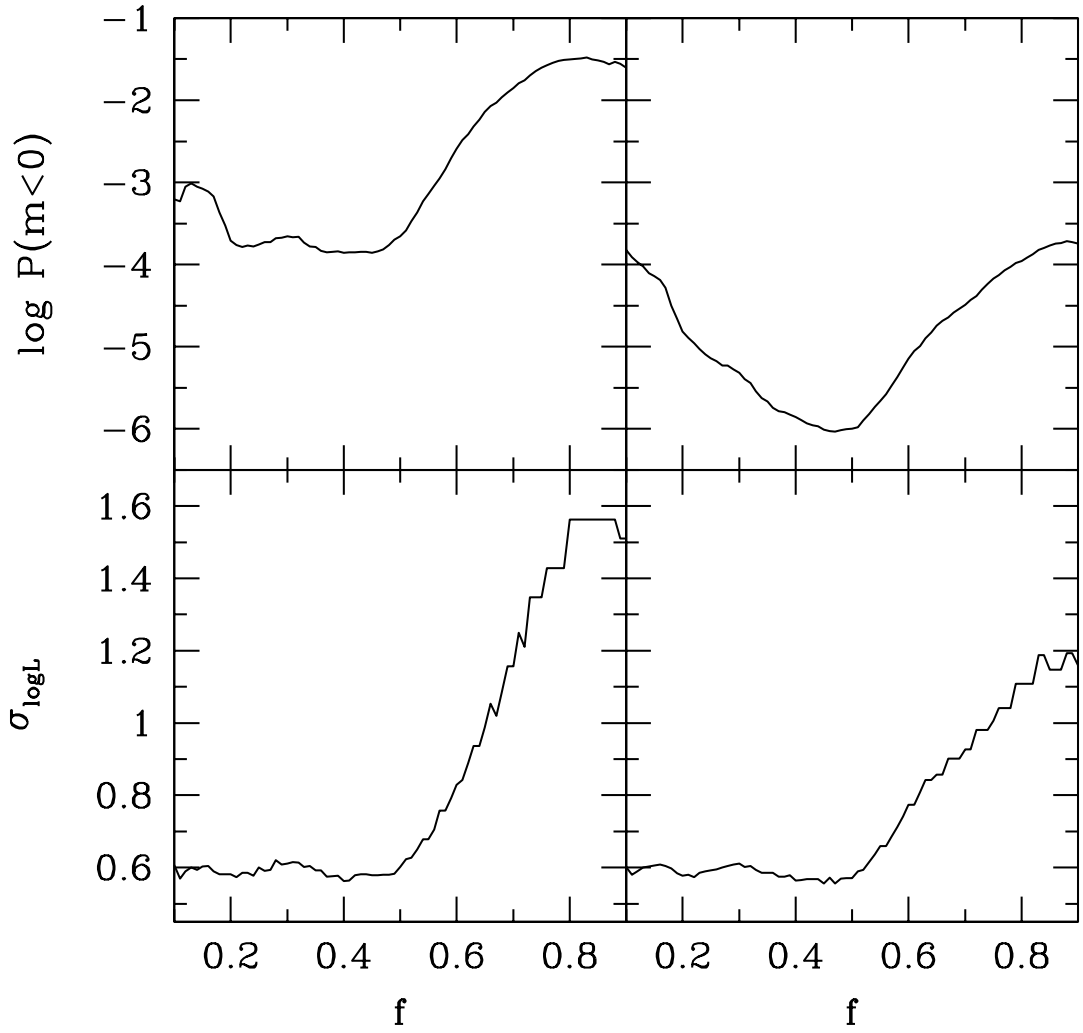

FIG. 7.—Probability $P(m < 0)$ that $m < 0$, as a function of f, and the extrinsic scatter $\sigma_{\log L}$ of the data along the $\log L$ axis as a function of f. In the left panels, we exclude GRB 980425 from the fits; in the right panels we include GRB 980425 in the fits.

the luminosity error bars in Figures 9 and 10 are dominated by this variation in the parameterization of the Band function, but they are clearly too small to matter. Hence, L is very insensitive to reasonable variations in the parameterization of the Band function for the bursts in our sample. The choice of source-frame energy range also is very unimportant: we chose 100–1000 keV to approximately match the observer-frame energy range in which BATSE measures peak fluxes, 50–300 keV, for redshifts typical of the bursts in our sample, $z \approx 1$–2.

4. THE LUMINOSITY ESTIMATOR

We list our sample of 20 bursts in Table 1; it consists of every burst for which redshift information is currently available. Peak fluxes are available for all 20 bursts. Spectroscopic redshifts and light curves of 64 ms or better resolution are available for 11 bursts. Spectroscopic redshifts and light curves of only 1 s resolution are available for two bursts. We compute variability lower limits for these bursts: we compute variabilities from their light curves without further degrading the effective resolution of these light curves by smoothing them on the 64 ms source-frame timescale (§ 2); these variabilities are lower limits to the variabilities that we would compute if 64 ms or better resolution light curves were available. Redshift upper limits (1) from the nondetection of the Lyα forest in host galaxy spectroscopy, in the case of one burst, and (2) from the nondetection of the Lyman limit in afterglow and host galaxy photometry, in the case of six bursts, and 64 ms or better resolution light curves are available for the remaining seven bursts. We compute luminosity upper limits for these bursts. We compute variabilities for these bursts for both $z = 0$ and z equal to the redshift upper limit; for all seven bursts, both of these variabilities are nearly identical, testifying to the weakness of the computational dependence of the variability on redshift (§ 2). In addition to the data listed in Table 1, we used *Ulysses*/GRB data for GRBs 970228, 990712, and 991208 to test the consistency of our results across instruments; we find the measured variabilities and luminosities of these bursts to be fully consistent across instruments.

We now construct the luminosity estimator. First, we compute the variabilities, V_f, and the isotropic equivalent peak

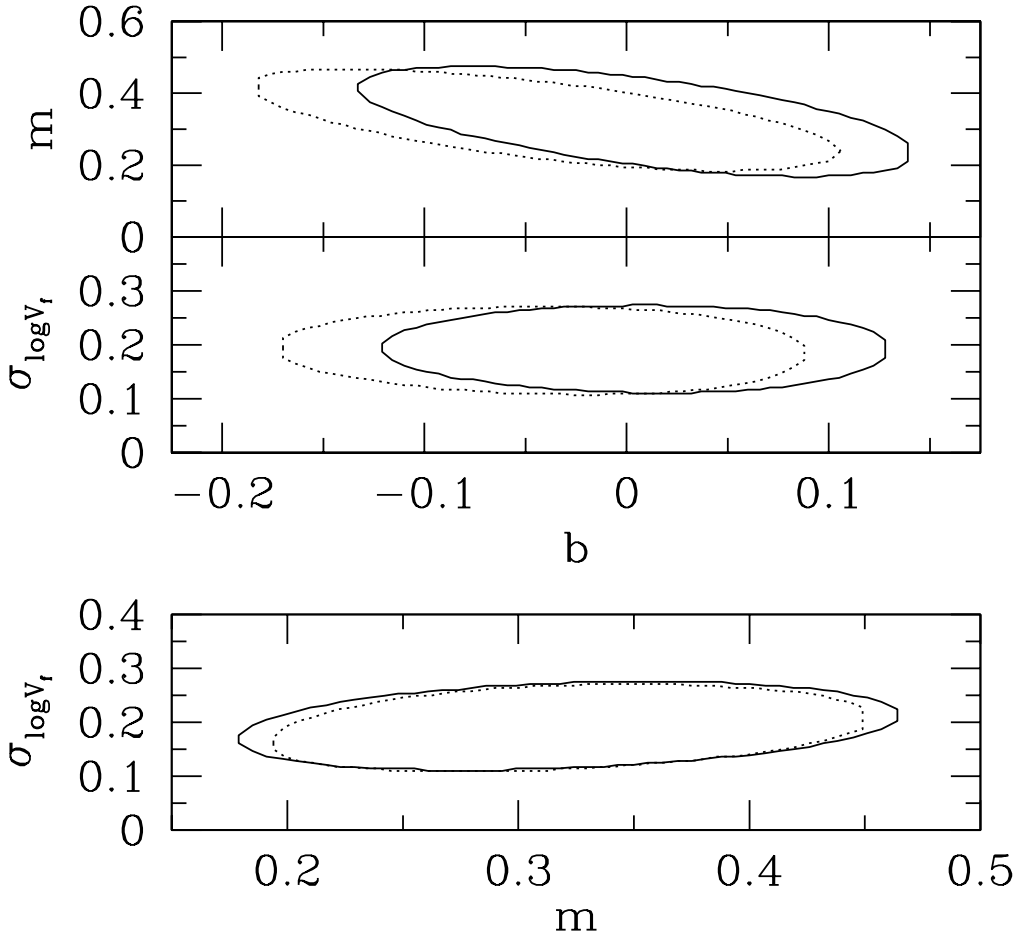

FIG. 8.—Two-dimensional uncertainty distributions of the fitted values of the model parameters b, m, and $\sigma_{\log V_f}$. Curves mark the 1 σ credible regions. Solid curves are for the case in which we exclude GRB 980425 from the fits ($f = 0.45$); dotted curves are for the case in which we include GRB 980425 in the fits ($f = 0.47$).

luminosities, L,[8] of the bursts in our sample. We compute the variabilities as functions of f, using the value of f to compute the smoothing timescales, T_f^E, of all the light curves in our sample (see § 1). We identify values of f that lead to successful and robust luminosity estimators below. Regardless of the value of f that we use to compute the variabilities, the distribution of our sample's bursts in the log L–log V_f plane appears to be well modeled by a normal distribution about a straight line (see, e.g., Fig. 9). We parameterize the line by

$$\log V_f(L) = \log \bar{V}_f + b + m(\log L - \log \bar{L}) , \tag{10}$$

where b is the intercept of the line, m is its slope, and $\bar{V}_f$ and $\bar{L}$ are the median values of V_f and L for the bursts in our sample for which spectroscopic redshifts, peak fluxes, and 64 ms or better resolution light curves are available. We parameterize this line as a function of L, instead of as a function of V_f, because the data do not fully rule out the possibility of $m \lesssim 0$, whereas they do rule out the possibility of very large values of m. We parameterize the normal distribution about this line by $\sigma_{\log V_f}$, which is half of the distribution's 1 σ width along the log V_f axis. Applying the Bayesian inference formalism developed by Reichart (2001) for fitting data with extrinsic scatter (in this case, $\sigma_{\log V_f}$) to data with intrinsic scatter (in this case, the uncertainties in the measured values of V_f and L), we determine values and uncertainties for the model parameters (b, m, and $\sigma_{\log V_f}$) as functions of f (Fig. 6).[9]

Of the 20 bursts in our sample, GRB 980425 is unique because of its possible association with SN 1998bw (Kulkarni et al. 1998b; Galama et al. 1998) at a redshift of $z = 0.0085$ (Tinney et al. 1998); the 12 other bursts for which spectroscopic redshifts are available have $0.430 < z < 3.418$. Consequently, we first construct the luminosity estimator excluding GRB 980425 from the above fits; we then repeat the fits including this burst. Excluding GRB 980425 from the fits, we first identify values of f that lead to successful and robust luminosity estimators. One measure of the success of a luminosity estimator is the probability that its slope, m, departs from $m = 0$. Since the best-fit values of m are positive (Fig. 6), we compute and plot in Figure 7 the

[8] We use peak fluxes measured on a 1 s timescale, and we take $H_0 = 65$ km s^{-1} Mpc^{-1}, $\Omega_m = 0.3$, and $\Omega_\Lambda = 0.7$; the luminosity estimator is very insensitive to these choices.

[9] This Bayesian inference formalism deals only with measurements with Gaussian error distributions, not with lower or upper limits. However, this formalism can be straightforwardly generalized to deal with limits as well, using two facts: (1) a limit can be given by the convolution of a Gaussian distribution and a Heaviside function; and (2) convolution is associative. In this paper, we fit to both measurements and limits.

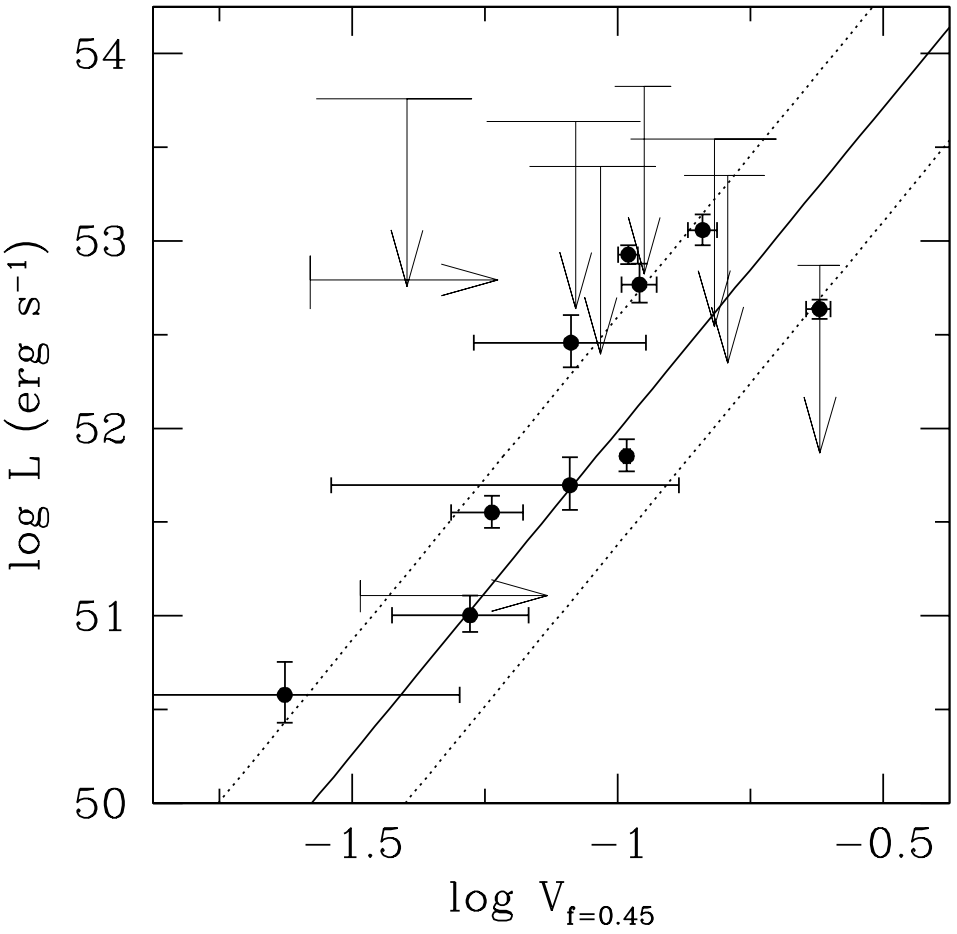

FIG. 9.—Variabilities $V_{f=0.45}$ and isotropic equivalent peak luminosities L of the bursts in our sample, excluding GRB 980425. Solid and dotted lines mark the center and 1 σ widths of the best-fit model distribution of these bursts in the log L–log $V_{f=0.45}$ plane.

probability that $m < 0$, $P(m < 0)$, as a function of f. We find that values of f between ≈ 0.2 and ≈ 0.5 lead to luminosity estimators with slopes that are positive with approximately equal probability: $P(m < 0) \approx 1.4 \times 10^{-4}$ (3.8 σ). Values of $f \lesssim 0.2$ and $f \gtrsim 0.5$ lead to luminosity estimators with slopes that are positive with increasingly less probability. In addition to having a slope that is positive (or negative) with large probability, a successful luminosity estimator also should be robust: small changes in the value of f should lead to only small changes in the estimated values of L. Consequently, we also plot in Figure 7 the extrinsic scatter of the data along the log L axis, $\sigma_{\log L} = \sigma_{\log V_f}/m$, as a function of f; this function is a measure of the maximum amount that the estimated luminosities of the bursts in our sample can change as a function of f. We find that values of $f \gtrsim 0.5$ lead to increasingly less robust luminosity estimators. Taking $f = 0.45$, which corresponds to the minimum in $P(m < 0)$, we compute smoothing timescales, $T_f^{E_i}$, for each of the instrument's available energy bands, E_i (Table 2), and using these smoothing timescales, we find that $\log \bar{V}_f = -1.088$, $\log \bar{L} = 51.852$, $b = 0.013^{+0.075}_{-0.092}$, $m = 0.302^{+0.112}_{-0.075}$, and $\sigma_{\log V_f} = 0.175^{+0.073}_{-0.046}$. Hence, we find that $L \sim V^{3.3^{+1.1}_{-0.9}}_{f=0.45}$. We plot the two-dimensional uncertainty distributions of the fitted values of the model parameters in Figure 8. We plot the data and the best-fit model of the distribution of these data in the log L–log V_f plane for $f = 0.45$ in Figure 9.

Although the solid line in Figure 9 is a good approximation of the best estimate for L as a function of V_f, the dotted lines in Figure 9 do not correspond to the uncertainty in L as a function of V_f. Those lines mark the best-fit width, given by $\sigma_{\log V_f} = 0.175$, of the best-fit model of the distribution of the data in the log L–log V_f plane; they do not account for the uncertainties in the fitted values of the model parameters, particularly those of b and m. Applying the Bayesian inference formalism of Reichart (2001), we formally compute the best estimate for L as a function of V_f and the uncertainty in L as a function of V_f, which we plot as solid curves in Figure 10. The computation of this distribution in the log L–log V_f plane is numerically intensive, so we also provide analytic approximations to these functions, which we plot as the dotted curves in Figure 10. The best estimate for L as a function of V_f can be approximated by equation (10), using the best-fit values of the model parameters. Approximating the uncertainty distributions of the fitted values of the model parameters (Fig. 8) as uncorrelated and Gaussian, the uncertainty in L as a function of V_f can be approximated by

$$\sigma_{\log V_f}(L) = \sqrt{\sigma^2_{\log V_f} + \sigma_b^2 + \sigma_m^2(\log L - \log \bar{L})^2} \tag{11}$$

(Reichart 2001), where $\sigma_{\log V_f}(L)$ is the 1 σ uncertainty in V_f as a function of L, $\sigma_{\log V_f} = 0.175$, $\sigma_b \approx 0.084$ is the uncertainty in the fitted value of b, and $\sigma_m \approx 0.094$ is the uncertainty in the fitted value of m. At its best, the luminosity estimator constructed

TABLE 1

REDSHIFTS, LUMINOSITIES, AND VARIABILITIES

GRB	z	L[a]	$V_{f=0.45}$	Instrument	z Reference
970228.....	0.695	$(5.0 \pm 1.7) \times 10^{51}$	0.08 ± 0.05	*Wind*/Konus	Djorgovski et al. 1999b
970508.....	0.835	$(1.0 \pm 0.2) \times 10^{51}$	0.05 ± 0.02	*CGRO*/BATSE	Metzger et al. 1997
970828.....	0.958	$(7.1 \pm 1.4) \times 10^{51}$	0.10 ± 0.00	*CGRO*/BATSE	Djorgovski 1999
971214.....	3.418	$(5.8 \pm 1.4) \times 10^{52}$	0.11 ± 0.01	*CGRO*/BATSE	Kulkarni et al. 1998a
980308.....	<4.3[b]	$<7.4 \times 10^{52}$	0.24 ± 0.02	*CGRO*/BATSE	Schaefer et al. 1999
980326.....	<4.3[b]	$<2.5 \times 10^{53}$	0.09 ± 0.02	*CGRO*/BATSE	Groot et al. 1998
980329.....	<3.9[c]	$<5.7 \times 10^{53}$	0.04 ± 0.01	*CGRO*/BATSE	Djorgovski 1999
980425.....	0.0085	$(5.2 \pm 2.0) \times 10^{46}$	0.00 ± 0.01	*CGRO*/BATSE	Tinney et al. 1998
980519.....	<4.3[b]	$<2.2 \times 10^{53}$	0.16 ± 0.03	*CGRO*/BATSE	Halpern et al. 1999
980613.....	1.096	$(1.3 \pm 0.2) \times 10^{51}$	>0.03[d]	*CGRO*/BATSE	Djorgovski et al. 1999c
980703.....	0.967	$(3.6 \pm 0.7) \times 10^{51}$	0.06 ± 0.01	*CGRO*/BATSE	Djorgovski et al. 1998
981220.....	<4.3[b]	$<4.3 \times 10^{53}$	0.08 ± 0.03	*Wind*/Konus	Masetti et al. 1998
990123.....	1.600	$(8.5 \pm 1.0) \times 10^{52}$	0.10 ± 0.00	*CGRO*/BATSE	Kulkarni et al. 1999
990510.....	1.619	$(4.3 \pm 0.5) \times 10^{52}$	0.24 ± 0.01	*CGRO*/BATSE	Beuermann et al. 1999
990705.....	< 5.5[b]	$<3.5 \times 10^{53}$	0.15 ± 0.05	*Ulysses*/GRB	Masetti et al. 2000
990712.....	0.430	$(3.8 \pm 1.5) \times 10^{50}$	0.02 ± 0.03	*Wind*/Konus	Galama et al. 1999
991208.....	0.706	$(2.9 \pm 1.0) \times 10^{52}$	0.08 ± 0.03	*Wind*/Konus	Djorgovski et al. 1999a
991216.....	1.020	$(1.1 \pm 0.2) \times 10^{53}$	0.14 ± 0.01	*CGRO*/BATSE	Vreeswijk et al. 1999
000131.....	<5.5[b]	$<6.7 \times 10^{53}$	0.11 ± 0.01	*Wind*/Konus	Pedersen et al. 2000
000301.....	2.034	$(6.2 \pm 2.0) \times 10^{52}$	>0.03[d]	*NEAR*/XGRS[e]	Castro et al. 2000

[a] Isotropic equivalent peak photon luminosity in ergs s^{-1} between source-frame energies 100 and 1000 keV, for peak fluxes measured on a 1 s timescale, $H_0 = 65$ km s^{-1} Mpc^{-1}, $\Omega_m = 0.3$, and $\Omega_\Lambda = 0.7$; upper limits are 1 σ.

[b] From nondetection of Lyman limit in afterglow or host galaxy photometry.

[c] From nondetection of Lyα forest in host galaxy spectroscopy.

[d] Only 1 s resolution light curve is available; lower limit is 1 σ.

[e] Peak flux from *Ulysses*/GRB.

TABLE 2

SMOOTHING TIMESCALES

GRB	Instrument[a]	$T^{E_1}_{f=0.45}$[b]	$T^{E_2}_{f=0.45}$[b]	$T^{E_3}_{f=0.45}$[b]	$T^{E_4}_{f=0.45}$[b]
970228.....	*Wind*/Konus	3.235	2.891	1.061	...[c]
970508.....	*CGRO*/BATSE	3.711	3.114	2.944	1.333
970828.....	*CGRO*/BATSE	19.057	15.875	12.335	11.276
971214.....	*CGRO*/BATSE	7.769	6.706	5.943	2.080
980308.....	*CGRO*/BATSE	4.987	6.135	4.903	...[d]
980326.....	*CGRO*/BATSE	0.782	0.836	...[e]	...[d]
980329.....	*CGRO*/BATSE	5.371	5.033	4.769	4.382
980425.....	*CGRO*/BATSE	7.819	6.701	5.169	0.839
980519.....	*CGRO*/BATSE	8.286	7.232	4.742	2.872
980613.....	*CGRO*/BATSE	8.160	8.432	6.528	...[d]
980703.....	*CGRO*/BATSE	18.024	16.659	15.191	11.733
981220.....	*Wind*/Konus	2.152	1.871	0.740	...[c]
990123.....	*CGRO*/BATSE	22.673	19.346	13.340	7.345
990510.....	*CGRO*/BATSE	6.911	4.964	3.118	...[d]
990705.....	*Ulysses*/GRB	4.986	...[f]	...[f]	...[f]
990712.....	*Wind*/Konus	2.405	3.595	0.925	...[c]
991208.....	*Wind*/Konus	7.737	4.682	4.299	...[c]
991216.....	*CGRO*/BATSE	4.641	3.842	2.905	2.009
000131.....	*Wind*/Konus	6.151	4.632	2.810	...[c]
000301.....	*NEAR*/XGRS	1.552	...[f]	...[f]	...[f]

[a] *CGRO*/BATSE: 25 keV $\lesssim E_1 \lesssim$ 55 keV, 55 keV $\lesssim E_2 \lesssim$ 110 keV, 110 keV $\lesssim E_3 \lesssim$ 320 keV, $E_4 \gtrsim$ 320 keV; *Wind*/Konus: 10 keV $\lesssim E_1 \lesssim$ 45 keV, 45 keV $\lesssim E_2 \lesssim$ 190 keV, 190 keV $\lesssim E_3 \lesssim$ 770 keV; *Ulysses*/GRB: 22 keV $\lesssim E_1 \lesssim$ 150 keV; *NEAR*/XGRS: 300 keV $\lesssim E_1 \lesssim$ 1000 keV.

[b] 45% smoothing timescale in seconds of light curve in observer-frame energy band E_i.

[c] Only three energy bands are available for this instrument.

[d] The smoothing timescale of the light curve in this energy band is less than the imposed effective sampling timescale of the light curve because of negligible emission in this energy band; consequently, we drop this energy band.

[e] There is an unusual, positive, constant, systematic offset of a portion of the light curve in this energy band; consequently, we drop this energy band.

[f] Only one energy band is available for this instrument.

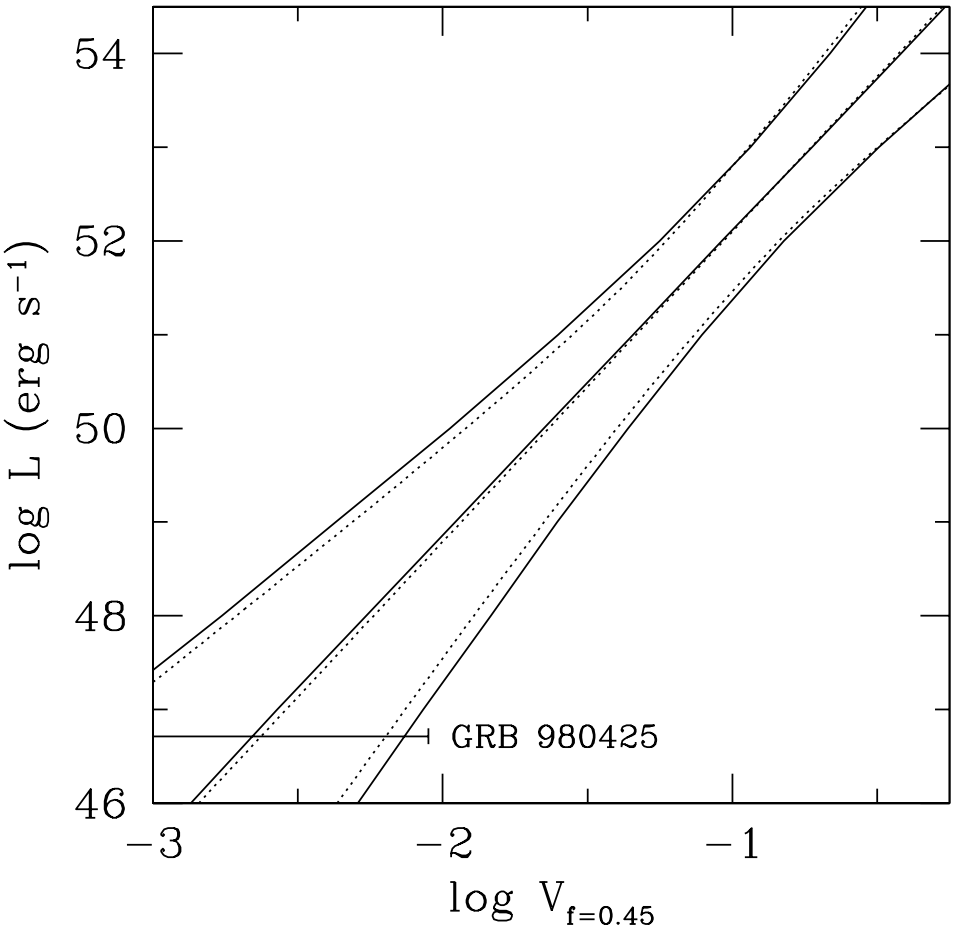

FIG. 10.—*Solid lines*: Best estimate for L as a function of $V_{f=0.45}$ and the 1 σ uncertainty in L as a function of $V_{f=0.45}$, when GRB 980425 is excluded from the fits. *Dotted lines*: analytic approximations to these functions, given by eqs. (10) and (11) and the fitted values of the model parameters. Clearly, GRB 980425 is consistent with the fitted model.

excluding GRB 980425 from the fits yields best-estimate luminosities that are accurate to a factor of ≈ 4, or best-estimate luminosity distances that are accurate to a factor of ≈ 2.

In addition to being used to estimate the luminosities of bursts for which spectroscopic redshifts are not available and the uncertainties in these luminosities, Figure 10 also can be used to determine if other bursts for which spectroscopic redshifts are available, such as GRB 980425 or future bursts, are consistent with the above fitted model. Consequently, we also plot GRB 980425 in Figure 10. Although its implied luminosity, $L = (5.2 \pm 2.0) \times 10^{46}$ ergs s^{-1}, is $\approx$4–6 orders of magnitude less

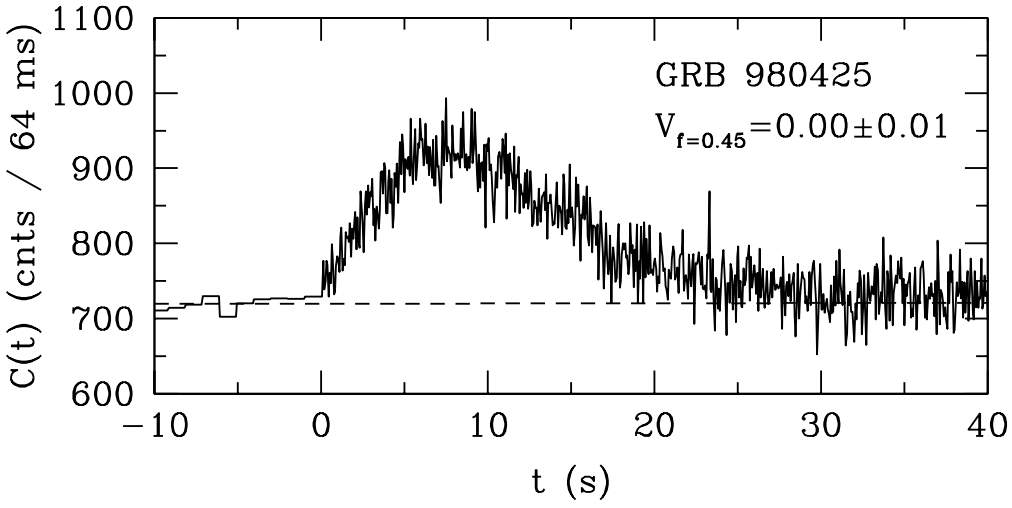

FIG. 11.—The >25 keV BATSE light curve of GRB 980425. We find that $V_{f=0.45} = 0.00 \pm 0.01$.

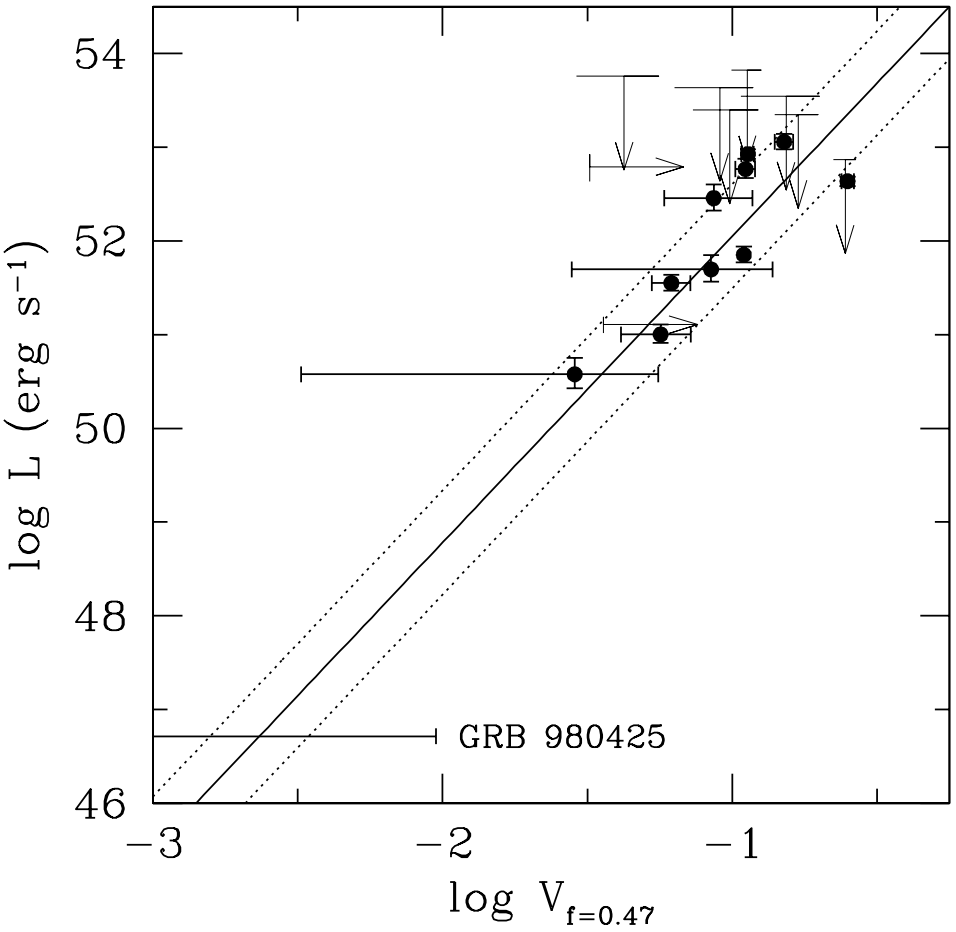

FIG. 12.—Variabilities $V_{f=0.47}$ and isotropic equivalent peak luminosities L of the bursts in our sample, including GRB 980425. Solid and dotted lines mark the center and 1 σ widths of the best-fit model distribution of these bursts in the log L–log $V_{f=0.47}$ plane.

than the 12 other measured luminosities of bursts in our sample, its variability, $V_{f=0.45} = 0.00 \pm 0.01$, also is considerably less than the ≈ 17 other reasonably well-constrained variabilities of bursts in our sample and clearly is consistent with the above fitted model. We plot the >25 keV BATSE light curve of GRB 980425 in Figure 11. Repeating the fits including GRB 980425 yields $f = 0.47$, $\log \bar{V}_f = -1.073$, $\bar{L} = 51.697$, $b = -0.035^{+0.080}_{-0.089}$, $m = 0.306^{+0.099}_{-0.071}$, $\sigma_{\log V_f} = 0.170^{+0.074}_{-0.041}$, and $P(m < 0) = 9.3 \times 10^{-7}$ (4.9 σ) (Figs. 6 and 7). Hence, we find that $L \sim V^{3.3^{+1.0}_{-0.8}}_{f=0.47}$. We also plot the two-dimensional uncertainty distributions of the fitted values of the model parameters in Figure 8. We plot the data and the best-fit model of the distribution of these data in the log L–log V_f plane for $f = 0.47$ in Figure 12. We plot the best estimate for L as a function of V_f, the uncertainty in L as a function of V_f, and our analytic approximations to these functions, given by equations (10) and (11) and the fitted values of the model parameters, in Figure 13.

5. DISCUSSION AND CONCLUSIONS

We have presented a rigorously constructed measure of the variability of a burst's light curve. Using this variability measure and a sample of 20 bursts, consisting of every burst for which redshift information is currently available, we have shown that a significant correlation exists between the variability of a burst's light curve and the burst's isotropic equivalent peak photon luminosity. This correlation between variability and luminosity is in agreement with the trends found by Stern et al. (1999) and Fenimore & Ramirez-Ruiz (2000). That is, more variable ("complex" in the terminology of Stern et al. 1999) bursts are more luminous, while less variable ("simple" in the terminology of Stern et al. 1999) bursts are less luminous.[10]

[10] However, we must draw attention to a potential disagreement between the primary conclusion of Stern et al. (1999) and the width of the luminosity distribution of the multiply peaked bursts with spectroscopically measured redshifts in our sample. Stern et al. (1999) find that the differential peak count rate distribution of their complex, or multiply peaked, BATSE bursts peaks about a factor of 4 above threshold, while the differential peak count rate distribution of their simple, or singly peaked, BATSE bursts does not have a similar peak. They interpret this to mean that their complex bursts are more luminous and at higher redshifts than their simple bursts: they argue that this peak corresponds to the peak in the star formation history of the universe at $z \sim 1.5$ and that it is not a threshold effect. However, as this peak is narrow, spanning less than an order of magnitude, this could be the case only if the luminosity function of the complex bursts is similarly narrow; otherwise, this feature would be washed out. We have visually examined the light curves of the bursts with spectroscopically measured redshifts in our sample, and we find that only GRB 980425 and GRB 970508 appear to be singly peaked. The remaining, multiply peaked bursts span ≈ 2.5 orders of magnitude, which appears to contradict Stern et al.'s interpretation of the peak that they find in the differential peak count rate distribution of their complex bursts.

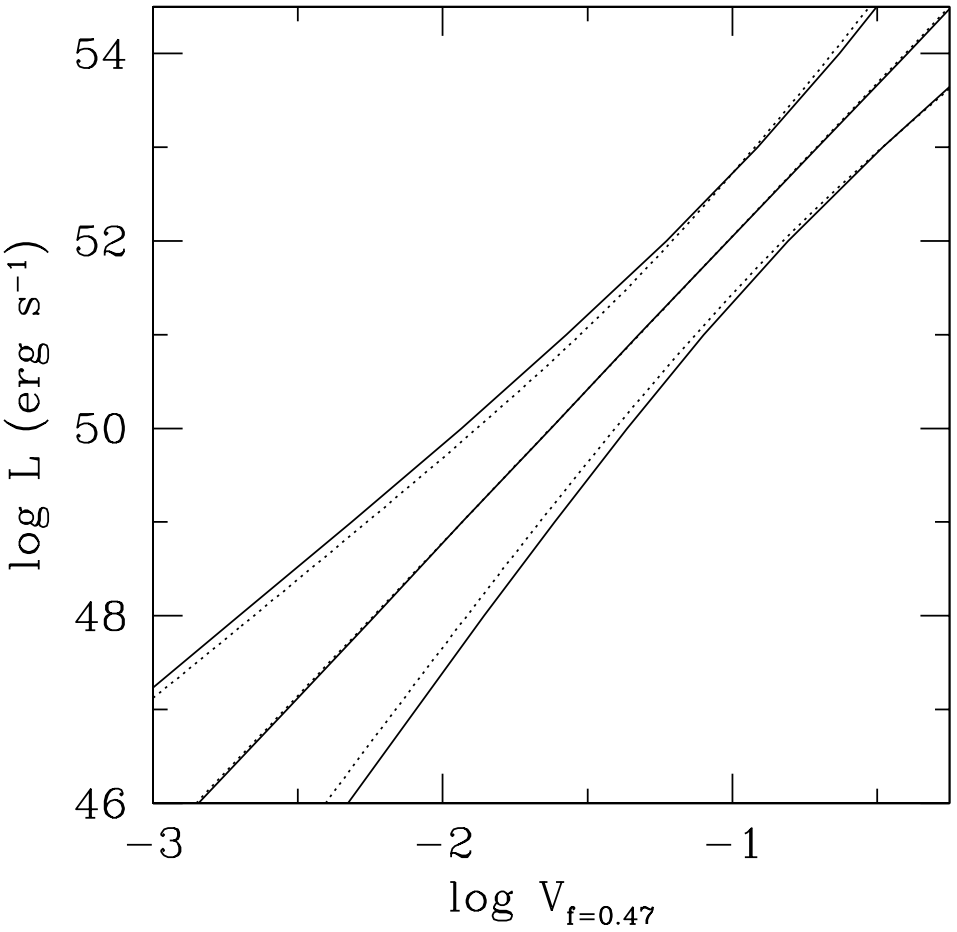

FIG. 13.—*Solid lines*: Best estimate for L as a function of $V_{f=0.47}$ and the 1 σ uncertainty in L as a function of $V_{f=0.47}$, when GRB 980425 is included in the fits. *Dotted lines*: Analytic approximations to these functions, given by eqs. (10) and (11) and the fitted values of the model parameters.

Furthermore, from the correlated variabilities and luminosities of our sample of 20 bursts, we have constructed a possible Cepheid-like luminosity estimator for the long bursts. If one excludes GRB 980425 from the fits, the luminosity estimator spans ≈ 2.5 orders of magnitude in luminosity, and its slope is positive with a probability of $1 - (1.4 \times 10^{-4})$ (3.8 σ). GRB 980425, however, is consistent with the fitted model. If one includes this burst in the fits, the luminosity estimator spans ≈ 6.3 orders of magnitude in luminosity, and its slope is positive with a probability of $1 - (9.3 \times 10^{-7})$ (4.9 σ).

Future bursts will either increase these probabilities or, possibly, disprove the luminosity estimator. However, because the uncertainty in L as a function of V_f in Figures 10 and 13 is dominated by extrinsic scatter (i.e., $\sigma_{\log V_f}$) and not by the uncertainties in the fitted values of the model parameters, a larger sample of bursts is unlikely to improve the predictive power of the luminosity estimator. Currently, the luminosity estimator yields best-estimate luminosities that are accurate to a factor of ≈ 4, or best-estimate luminosity distances that are accurate to a factor of ≈ 2.

However, whether or not the luminosity estimator is eventually disproved, the light curve of GRB 980425 is unique in that it is much less variable than the other ≈ 17 light curves of bursts in our sample for which the signal-to-noise ratio is reasonably good: $\log V_{f=0.45} < -1.5$ with a probability of $1 - (3.4 \times 10^{-4})$ (3.4 σ) and $\log V_{f=0.45} < -1$ with a probability of $1 - (3.5 \times 10^{-23})$ (9.9 σ). The argument has been made that the association of GRB 980425 with SN 1998bw at the unusually low redshift of $z = 0.0085$ is probably accidental because the light curve of GRB 980425 is no different than the light curves of the cosmological bursts. On the contrary, we find that the light curve of GRB 980425 is different from the light curves of the cosmological bursts. Consequently, GRB 980425 may well be associated with SN 1998bw.

If GRB 980425 is associated with SN 1998bw and if the luminosity estimator is correct, the fact that GRB 980425 is consistent with the fitted model suggests that GRB 980425 and the cosmological bursts may share a common, or at least a related, physical origin, although they cannot share a common redshift distribution and/or luminosity function (Graziani, Lamb, & Marion 1999). This conclusion is made more intriguing by the recent discoveries of supernova-like components in the late afterglows of the cosmological bursts GRB 970228 (Reichart 1999, Galama et al. 2000; Reichart, Castander, & Lamb 2000; Reichart, Lamb, & Castander 2000) and GRB 980326 (Bloom et al. 1999).

Support for this work was provided by NASA through the Hubble Fellowship grant HST-SF-01133.01-A from the Space Telescope Science Institute, which is operated by the Association of Universities for Research in Astronomy, Inc., under NASA contract NAS 5-26555. Support for this work was also provided by NASA contracts NAS W-4690 and SCSV 464006. K. H. acknowledges *Ulysses* support under JPL Contract 958056. We are very grateful to Evgeny Mazets and the Konus

team for granting us the use of their data. We are also grateful to Paul Butterworth for retrieving the Konus data and to Marc Kippen for retrieving the BATSE data for GRB 980613. We also thank Carlo Graziani for generously sharing his insights into Bayesian inference. Finally, D. E. R. thanks Bob Nichol and the Department of Physics at Carnegie Mellon University, and Bernard and Marilyn Keisler for their hospitality during the summer of 2000.

REFERENCES

Band, D., et al. 1993, ApJ, 413, 281
Beuermann, K., et al. 1999, A&A, 352, L26
Bloom, J. S., et al. 1999, Nature, 401, 453
Castro, S. M., Dierks, A., Kulkarni, S. R., Djorgovski, S. G., Scoville, N. Z., & Frayer, D. T. 2000, GCN Circ. 605 (http://gcn.gsfc.nasa.gov/gcn/gcn3/605.gcn3)
Costa, E., et al. 1997, Nature, 387, 783
Djorgovski, S. G. 1999, report, paper presented at Santa Barbara Institute for Theoretical Physics Workshop on Gamma-Ray Bursts, 1999 March 15–19
Djorgovski, S. G., Dierks, A., Bloom, J. S., Kulkarni, S. R., Filippenko, A. V., Hillenbrand, L. A., & Carpenter, J. 1999a, GCN Circ. 481 (http://gcn.gsfc.nasa.gov/gcn/gcn3/481.gcn3)
Djorgovski, S. G., Kulkarni, S. R., Bloom, J. S., & Frail, D. A. 1999b, GCN Circ. 289 (http://gcn.gsfc.nasa.gov/gcn/gcn3/289.gcn3)
Djorgovski, S. G., Kulkarni, S. R., Bloom, J. S., Frail, D. A., Chaffee, F., & Goodrich, R. 1999c, GCN Circ. 189 (http://gcn.gsfc.nasa.gov/gcn/gcn3/189.gcn3)
Djorgovski, S. G., Kulkarni, S. R., Bloom, J. S., Goodrich, R., Frail, D. A., Piro, L., & Palazzi, E. 1998, ApJ, 508, L17
Fenimore, E. E., & Ramirez-Ruiz, E. 2000, ApJ, submitted (astro-ph/0004176)
Fenimore, E. E., in't Zand, J. J. M., Norris, J. P., Bonnell, J. T., & Nemiroff, R. J. 1995, ApJ, 448, L101
Frail, D. A., Kulkarni, S. G., Nicastro, L., Feroci, M., & Taylor, G. B. 1997, Nature, 389, 261
Galama, T. J., et al. 1998, Nature, 395, 670
———. 1999, GCN Circ. 388 (http://gcn.gsfc.nasa.gov/gcn/gcn3/388.gcn3)
———. 2000, ApJ, 536, 185
Graziani, C., Lamb, D. Q., & Marion, G. H. 1999, A&AS, 138, 469
Groot, P. J., et al. 1998, ApJ, 502, L123
Halpern, J. P., Kemp, J., Piran, T., & Bershady, M. A. 1999, ApJ, 517, L105
Klebesadel, R. W., Strong, I. B., & Olson, R. A. 1973, ApJ, 182, L85
Kulkarni, S. R., et al. 1998a, Nature, 393, 35
———. 1998b, Nature, 395, 663
Kulkarni, S. R., et al. 1999, Nature, 398, 389
Masetti, N., et al. 1998, GCN Circ. 179 (http://gcn.gsfc.nasa.gov/gcn/gcn3/179.gcn3)
———. 2000, A&A, 354, 473
Metzger, M. R., Djorgovski, S. G., Kulkarni, S. R., Steidel, C. C., Adelberger, K. L., Frail, D. A., Costa, E., & Frontera, F. 1997, Nature, 387, 879
Norris, J. P., Marani, G. F., & Bonnell, J. T. 2000a, in AIP Conf. Proc. 526, Gamma-Ray Bursts: 5th Huntsville Symposium, ed. R. M. Kippen, R. S. Mallozzi, & G. J. Fishman (New York: AIP), 78
———. 2000b, ApJ, 534, 248
Paciesas, W. S., et al. 1999, ApJS, 122, 465
Pedersen, H., et al. 2000, GCN Circ. 534 (http://gcn.gsfc.nasa.gov/gcn/gcn3/534.gcn3)
Ramirez-Ruiz, E., & Fenimore, E. E. 1999, report, paper presented at the 5th Huntsville Symposium on Gamma-Ray Bursts
Reichart, D. E. 1999, ApJ, 521, L111
———. 2001, ApJ, in press (astro-ph/9912368)
Reichart, D. E., Castander, F. J., & Lamb, D. Q. 2000, in AIP Conf. Proc. 522, Cosmic Explosions: Tenth Astrophysics Conference, ed. S. S. Holt & W. W. Zhang (New York: AIP), 253
Reichart, D. E., et al. 2001, in preparation
Reichart, D. E., Lamb, D. Q., & Castander, F. J. 2000, in AIP Conf. Proc. 526, Gamma-Ray Bursts: 5th Huntsville Symposium, ed. R. M. Kippen, R. S. Mallozzi, & G. J. Fishman (New York: AIP), 414
Sahu, K. C., et al. 1997, Nature, 387, 476
Schaefer, B. E., et al. 1999, ApJ, 524, L103
Stern, B., Poutanen, J., & Svensson, R. 1999, ApJ, 510, 312
Stern, B., Svensson, R., & Poutanen, J. 1997, in 2d INTEGRAL Workshop: The Transparent Universe, ed. C. Winkler, T. J.-L. Courvoisier, & P. Durouchoux (ESA SP-382) (Paris: ESA), 473
Tinney, C., et al. 1998, IAU Circ. 6896
van Paradijs, J., et al. 1997, Nature, 386, 686
Vreeswijk, P. M., et al. 1999, GCN Circ. 496 (http://gcn.gsfc.nasa.gov/gcn/gcn3/496.gcn3)